Dissociative recombination of the cation and dication of CO_2

K. Seiersen, A. Al-Khalili,* O. Heber,† M. J. Jensen,‡ I. B. Nielsen, H. B. Pedersen,§ C. P. Safvan,‖ and L. H. Andersen
Department of Physics and Astronomy, University of Aarhus, DK-8000 Århus C, Denmark
(Received 6 February 2003; published 22 August 2003)

Dissociative recombination of CO_2 ions has been studied at the heavy-ion storage ring ASTRID. Electrons were scattered on both singly and doubly charged positive ions of the molecule, and the absolute cross sections were measured in the energy range of 10^{-3}–10^{1} eV. Thermal rate coefficients of $\alpha(CO_2^{+}) = (6.5 \pm 1.9) \times 10^{-7} \times (300/T[\mathrm{K}])^{0.8}$ cm^3 s^{-1} and $\alpha(CO_2^{2+}) = (6.2 \pm 2.1) \times 10^{-7} \times (300/T[\mathrm{K}])^{0.5}$ cm^3 s^{-1} were extracted. Furthermore, branching ratios for molecular breakup into neutral product channels have been measured using a grid technique. The branching ratios were measured at ~ 0 eV for CO_2^{+}, and in the entire energy range from 10^{-3} eV to 50 eV for CO_2^{2+}. This measurement reveals pronounced structure in the CO_2^{2+} branching ratios.

DOI: 10.1103/PhysRevA.68.022708 PACS number(s): 34.80.Ht, 34.80.Lx

INTRODUCTION

Dissociative recombination (DR) is the reaction in which a positively charged molecular ion recombines with an electron to form an excited intermediate complex, which subsequently dissociates into smaller fragments:

$$ABC^{n+} + e^{-} \rightarrow \{ABC^{(n-1)+}\}^{*} \rightarrow \text{Multichannel dissociation.} \quad (1)$$

The excited intermediate complex can be a dielectronically excited system (the *direct* DR mechanism [1]) or an electronically and vibrationally excited Rydberg system (the *indirect* DR mechanism [2]). DR is a complex molecular process that occurs in any plasma cold enough to contain molecular constituents. It is typically one of the dominant processes in both naturally occurring and man-made plasmas relevant not only to, e.g., planetary atmospheres [3,4], fusion plasmas [5], chemistry of interstellar matter [6–8], and the comas of comets [9], but also to laser physics, reentry vehicles, plasma processing, and combustion science. A review of dissociative recombination can be found in Refs. [10–12].

Experimental developments over the last couple of decades have made possible detailed studies on the structure and spectroscopy of *singly* charged molecular ions, and a substantial body of information now exists on positively charged diatomic and polyatomic molecules. However, despite the fact that long-lived *multiply* charged molecular ions have been observed in mass spectrometry experiments conducted over a period of more than 80 years [13,14], studies of such species continue to pose a significant theoretical and experimental challenge.

Multiply charged molecular cations differ from singly charged species in fundamental ways. The long-range Coulomb repulsion lifts the potential-energy surfaces as the internuclear distance is decreased. Small multiply charged ions are thus unstable towards dissociation because their energy levels are embedded in the continuum. The bonding properties of dications give rise to interesting topologies of their potential-energy surfaces: The short-range binding interactions within a molecule may form a local minimum in the otherwise repulsive Coulomb barrier, resulting in a metastable system. This system will eventually decay through either direct dissociation (preceded by tunneling through the barrier), or by electronic predissociation by another state.

The high density of electronic states encountered in many multiply charged molecular systems makes accurate calculations difficult and demands the use of *ab initio* quantum chemical methods well beyond the simple Hartree-Fock level. The relatively high energy required for their formation (at least 20–40 eV with respect to the neutral ground state) and the intrinsic instability of such ions complicate experiments [15,16].

Electron capture by multiply charged molecular ions has been proposed [17] as a mechanism for generating ions in the Earth's upper atmosphere. Molecular double photoionization has been proposed as a source of energetic, charged particles in the terrestrial ionosphere and in the interstellar medium [18]. Furthermore, multiply charged molecules may be found in various astrophysical environments [15,19].

The CO_2 molecule in particular has attracted much attention in the past two decades, primarily due to the importance of both the neutral and the ionized form in high-power lasers and in terrestrial and planetary atmospheres (CO_2 being the dominant molecular constituent in the atmospheres of both Mars and Venus). The molecule is quite abundant not only in the interstellar medium, especially as a solid component of frozen grain mantles, but also in the gaseous phase [21,22]. Furthermore, the dication of CO_2 has just recently been predicted (using results presented in this paper) to exist in the atmosphere of Mars in densities detectable by future space missions to the Mars [20].

Doubly charged positive ions have been known since 1899 with the discovery of atomic He^{2+} ions (α particles). The first multiply charged molecules were discovered by As-

*Present address: Stockholm University, AlbaNova University Center, Molecular Physics, SE-106 91, Stockholm, Sweden.
†Present address: Department of Particle Physics, Weizmann Institute of Science, Rehovot 76100, Israel.
‡Present address: National Institute of Standards and Technology, Boulder, CO 80305-3328, USA.
§Present address: Max-Planck-Institut für Kernphysik, 69117 Heidelberg, Germany.
‖Present address: Nuclear Science Center, P.O. Box 10502, Aruna Asaf Ali Marg, New Delhi 110067, India.

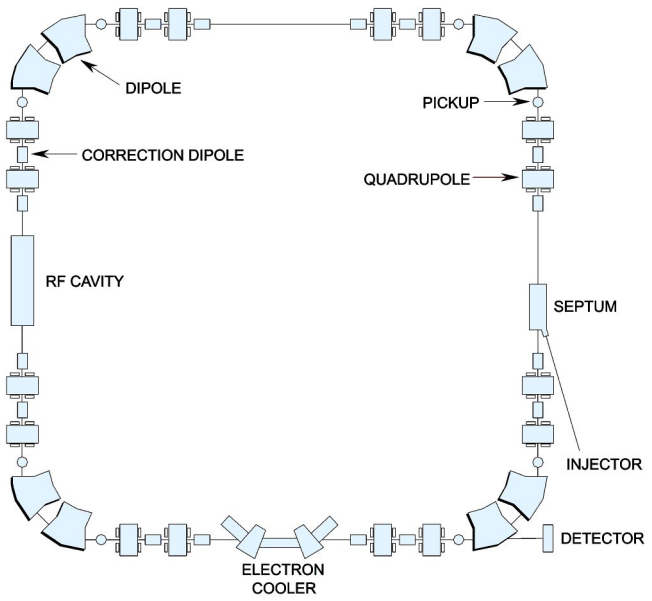

FIG. 1. Schematic diagram of the ASTRID heavy-ion storage ring. Ions are injected in the right hand side of the figure, circulating counterclockwise in the ring. The electron target is shown in the bottom of the figure, and in the dipole magnet following the electron target, the neutral detector is shown.

ton [13], and later Thomson [23] found evidence for N_2^{2+} or CO^{2+}. Later again, Conrad [14] identified several doubly charged ions, e.g., CO^{2+} and CO_2^{2+}; the latter being the subject of this paper. A metastable state of CO_2^{2+} was discovered in 1964 [24], and storage ring experiments about 10 years ago [25,26] on CO_2^{2+} and other dications showed that multiply charged positive ions can contain long-lived components with lifetimes longer than a few seconds. In the experiment it was found that the lifetime was limited by residual gas collisions, and the ions were practically stable, at least on the time scale of a storage ring experiment, which thus allowed further storage ring investigations of the ions, as presented in this paper. Today, even small thermodynamically stable dications, i.e., dications stable with respect to all dissociation channels, are known [27].

DR of CO_2^+ has been studied using both the stationary and the flowing afterglow techniques since 1967, but to the best of our knowledge, this is the first study of the CO_2^+ DR rate coefficient using the storage ring technique. Further, this is believed to be the first determination of the DR rate coefficient for CO_2^{2+}. DR measurements on CO^+ [28] and CO^{2+} [29] have been performed earlier.

EXPERIMENT

The present study comprises two independent experiments at the heavy-ion storage ring ASTRID [30] in Århus, Denmark. The ring has a square geometry with two 45° bending magnets in each of the four corners (see Fig. 1), and a total circumference of 40 m. In short, each experiment is composed of producing, storing, and accelerating the desired ions (in this case CO_2^+ and CO_2^{2+}), bombarding them with electrons of a particular energy, and extracting the cross section from the measured number of reactants and products.

Ions were produced by electron-impact ionization of a CO_2 gas in a Nielsen-type plasma ion source [31] and ion currents of about 1 μA of CO_2^+ and 60 nA of CO_2^{2+} were extracted. The ions were preaccelerated and mass selected by a 150-kV ion separator and then injected into the storage ring. The ions were further accelerated to the final storage energy by means of a radio-frequency acceleration system. CO_2^+ was stored at 3.35 MeV and CO_2^{2+} at 6.50 MeV. At these energies, the lifetimes, which were limited by collisions with the background gas in the ring, were 2 sec and 1 sec, respectively. The time spent in storing and accelerating the beam (several seconds) will normally allow the stored ions to decay to the electronic and vibrational ground states, but as both CO_2^+ and CO_2^{2+} ions have no dipole moment, some rovibrational excitation is believed to exist in the stored beams.

In one of the straight sections of the ring the ions were merged with an essentially mono-energetic electron beam, which was provided by an electron cooler [32]. Ions and electrons interact in an ≈ 1 m interaction region, and neutral particles created in this section are detected by an energy-sensitive surface-barrier-type solid-state detector (SSD) located *after* the bending, magnet following the interaction region. By chopping the electron beam, we can distinguish the neutrals created by background gas collisions from those created by ion-electron interactions.

If an event fully neutralizes the ion, the product fragments will deposit the full ion-beam energy in the SSD. This is for instance the case for dissociative recombination of a singly charged ion. For DR of a dication, however, a full neutralization of the ion (i.e., a double recombination) is very unlikely due to the relatively low-electron density in our experiment (10^6–10^7 cm^{-3}). In this case (and in the case of dissociative excitation), the reaction leads to the formation of both charged and neutral fragments. The neutrals will only deposit a fraction of the beam energy in the SSD, while the rest of the energy is carried away by the charged fragments. This is clearly seen in the two SSD pulse height spectra in Fig. 2: The full energy peak at mass 44, which is seen for the monocation, is missing in the dication spectrum. A small impurity peak at mass 24 was discovered in the spectrum. Though we could not identify this impurity, we were able to remove it before the actual experiment by switching to a different ion source. The impurity is believed to be due to a memory effect in the initial ion source. The peak is seen in Fig. 2, which demonstrates the power of ASTRID as a diagnostics tool for determining the constituent ions coming from the ion source, thus ensuring the correct ion target for the experiment.

Cross sections were measured as a function of the relative energy by varying the energy of the electrons while keeping the ion energy constant. This relative or center-of-mass energy E is related to the ion and electron energies in the laboratory frame, E_i and E_e, in the following way:

$$E=\frac{1}{2}m_e(v_i-v_e)^2=\left[\sqrt{\frac{m_e}{M_i}E_i}-\sqrt{E_e}\right]^2, \qquad (2)$$

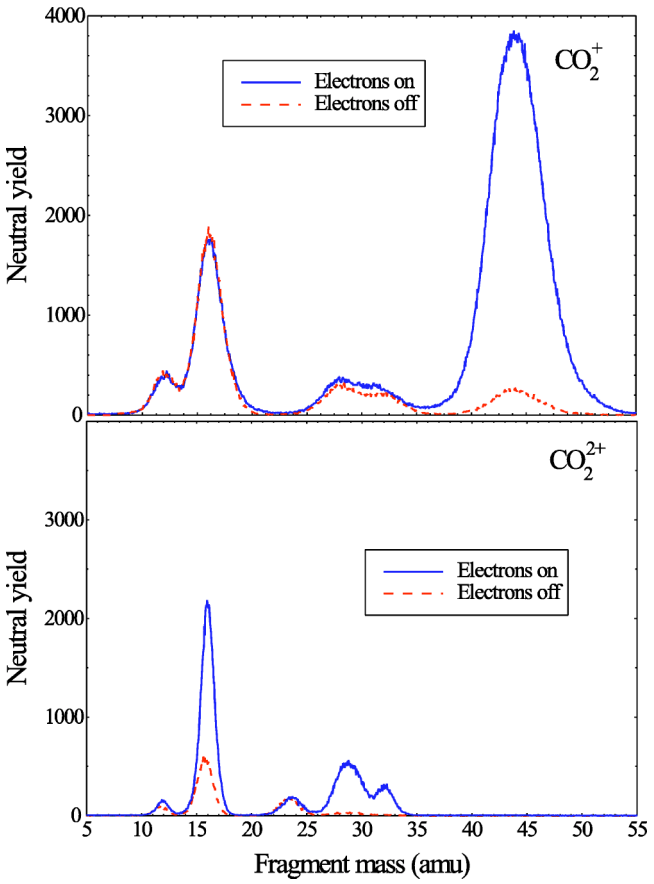

FIG. 2. Output from the energy-sensitive solid-state detector. Neutral fragments impacting the detector will result in a signal proportional to the energy carried by the particle. This makes it possible to distinguish between carbon atoms, oxygen atoms, and combinations of these. The spectrum shows the signal for both background induced and electron induced reactions.

where M_i and m_e are the ion and electron masses, and v_i and v_e are the ion and electron velocities. The absolute rate coefficient for a given process can be written in terms of measurable quantities as

$$\langle v\sigma\rangle = \frac{N_s - N_b}{N_{ion}} \frac{v_i}{n_e \Delta L \epsilon}, \tag{3}$$

where v is the relative velocity, σ is the cross section, v_i is the ion velocity, n_e is the electron density, ΔL is the length of the interaction region, and $\epsilon(=1)$ is the detection efficiency. N_s and N_b are the rates of neutrals (particles per second in a given detector energy window) recorded with the electron beam on and off, respectively. N_{ion} is the number of ions passing through the electron cooler per second.

Note that the relative ion-electron velocities in the toroid regions where the beams are merged are different from those inside the interaction region. This produces a small (less than a factor of 2) toroid contribution to the measured rate coefficients, but the data presented in this paper are all corrected for this.

In practice, we replace the rate of ions N_{ion} in Eq. (3) with the rate of background events, which is proportional to the number of ions in the ring, thus only measuring a relative rate coefficient. To put this relative measurement on an absolute scale, we choose one specific center-of-mass energy where we repeat our measurement, but with the correct absolute rate coefficient of ions inserted. This absolute rate coefficient was measured by two different methods. The CO_2^+ current was measured with a beam charge monitor (BCM) from Bergoz [33] capable of measuring ion currents down to ~50 nA with a resolution below 10 nA. The stored ion currents of CO_2^{2+} did not exceed 10 nA and the BCM technique could not be used. Instead we used the signal from a set of pick-up electrodes in ASTRID. This signal was fed to a spectrum analyzer that monitored the input at the revolution frequency of the ions, thus providing a measure of the number of ions in the ring. The signal was calibrated to a known ion current. For this method to be exact, the two ion beams (the calibration ion beam and the CO_2^{2+} beam) have to be stored with identical ion bunch shapes, which is not always guaranteed. We thus estimate the uncertainty of this technique to be about 30%. Indeed, the main contribution to the uncertainties of our results comes from the absolute measurement of the stored ion current.

RESULTS AND DISCUSSION

Cross sections

The total DR rate coefficients of the present experiment are shown in Fig. 3. What we measure is the signal in each of the peaks of the spectrum in Fig. 2. Without the grid method, to be described in the following section, we cannot distinguish the fragment identity in each of the peaks, i.e., the peak at mass 28, for instance, will contain both CO molecules and C+O atoms arriving simultaneously. Because of this, we only label the channels by the individual atoms in the channel in Fig. 3.

For CO_2^+, the rate coefficient is observed to drop two orders of magnitude up to a center-of-mass energy of about 1 eV. A wide resonance is seen at about 7 eV, and the rate coefficient then drops at higher energies. Above ≈10 eV we start to see dissociative excitation channels, i.e., channels containing charged fragments where not all constituent atoms of the molecule hit the detector. The CO_2^{2+} rate coefficients drop continuously up to 10 eV, and resonancelike structures are seen in the total rate coefficient at 0.3, 0.7, and 3 eV. Notice the sharp drop near 8 eV in the (C,O) channel (i.e., the SSD peak at mass 28), which will be discussed later in connection with branching ratios.

The electron distribution in the electron cooler is not equal to that of a thermal plasma [32]. It is an anisotropic velocity distribution, of which we estimate a longitudinal temperature of $kT=1$ meV, and a transversal temperature of $kT=25$ meV. To compare the measured rate coefficients to the thermal rate coefficients (which is the parameter relevant to plasma physics), the cross section must first be unfolded from the electron cooler velocity distribution and then reconvoluted with a thermal electron distribution; that is, we find σ from $\langle\sigma v\rangle_{cooler}$ and then calculate $\alpha=\langle\sigma v\rangle_{thermal}$.

In practice, we compare the measured rate coefficients with model cross sections that have been convoluted with the

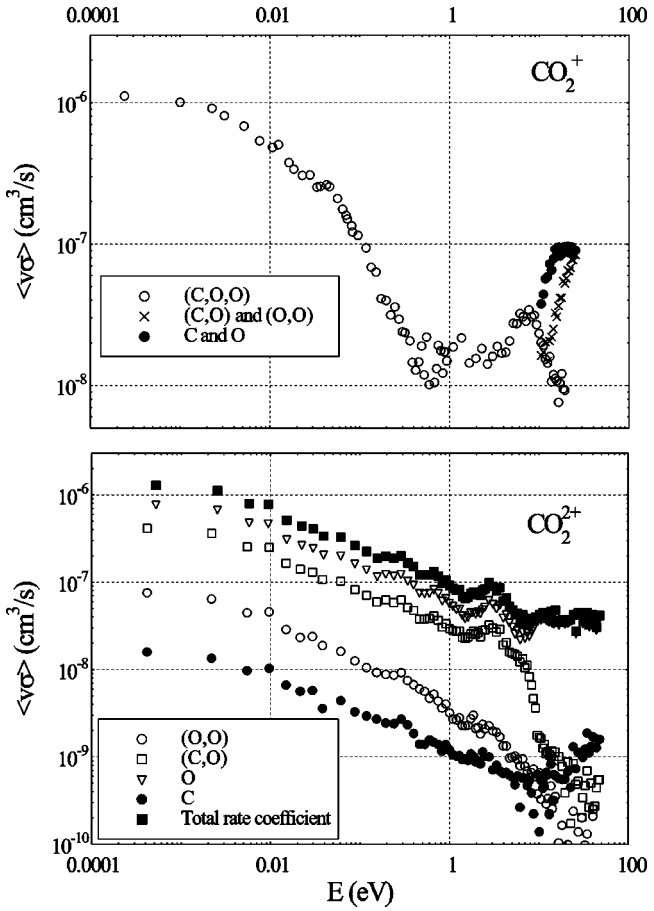

FIG. 3. Measured absolute rate coefficients for CO_2^+ and CO_2^{2+}. The curves show the different rate coefficients measured for each individual neutral fragment peak in Fig. 2. Each curve is denoted by the atomic constituents of the neutral particles. For instance, the curve denoted by "(C,O)" includes channels such as $(CO+O^+)$ and $(C+O+O^+)$.

known electron cooler velocity distribution. This yields the following cross sections (see Fig. 4 for the CO_2^+ data):

$$\sigma_{CO_2^+}(E) = 4\times10^{-16}\frac{1}{(E[\mathrm{eV}])^{1.3}}\ \mathrm{cm}^2,$$

$$\sigma_{CO_2^{2+}}(E) = 1.5\times10^{-15}\frac{1}{(E[\mathrm{eV}])}\ \mathrm{cm}^2. \qquad (4)$$

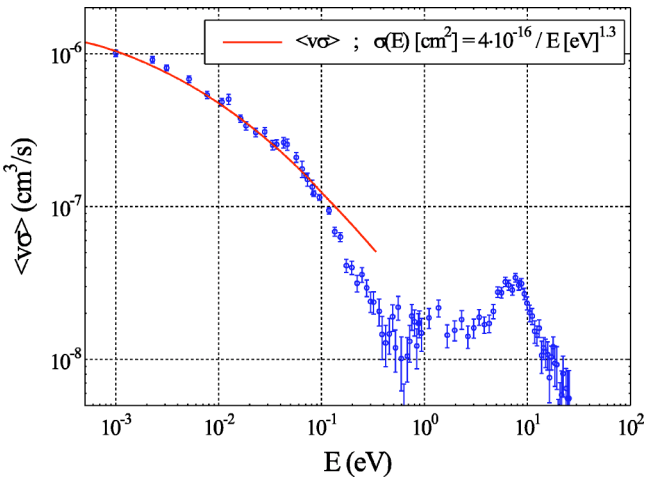

FIG. 4. Model cross section convoluted with electron cooler velocity distribution compared with measured $\langle v\sigma\rangle$ for CO_2^+. Measured data show good overlap with the model cross section in the energy range from 10^{-3} to 10^{-1} eV.

This allows us to extract a thermal DR rate coefficient in accordance with the relation [34]

$$\alpha(T) = \frac{8\pi m_e}{(2\pi m_e kT)^{3/2}}\int_0^\infty \sigma(E)e^{-E/kT}E\,dE. \qquad (5)$$

Using the cross sections given in Eq. (4), this integral can be calculated analytically, yielding the following rate coefficients:

$$CO_2^+ : (6.5\pm1.9)\times10^{-7}\times\left(\frac{300}{T[\mathrm{K}]}\right)^{0.8}\ \mathrm{cm}^3\,\mathrm{s}^{-1},$$

$$CO_2^{2+} : (6.2\pm2.1)\times10^{-7}\times\left(\frac{300}{T[\mathrm{K}]}\right)^{0.5}\ \mathrm{cm}^3\,\mathrm{s}^{-1}. \qquad (6)$$

This is to our knowledge the first measurement of the DR rate coefficient for the CO_2 dication. The DR rate coefficient for the monocation has, however, been measured before. Our result compares to previous stationary and flowing afterglow results as listed in Table I. It can be seen that the present data is almost a factor of 2 higher than previous measurements, yet we are still well within a two-standard-deviation range of these results. We cannot, however, rule out the possibility

TABLE I. Thermal rate coefficient ($T=300$ K) for DR of CO_2^+.

Method	Thermal rate coefficient ($\mathrm{cm}^3\,\mathrm{s}^{-1}$)	Reference
Microwave afterglow	$(3.8\pm0.5)\times10^{-7}$	[35] (1967)
Microwave afterglow	$(4.0\pm0.5)\times10^{-7}$	[36] (1973)
FALP[a]	$(3.1\pm0.6)\times10^{-7}$	[37] (1991)
FALP	$(3.5\pm0.5)\times10^{-7}$	[38] (1997)
Storage ring	$(6.5\pm1.9)\times10^{-7}$	This work

[a]FALP denotes flowing afterglow with Langmuir probe.

that remaining rovibrational excitation has some influence on the rate coefficient, which is not present in the afterglow experiments.

Branching ratios

The possible outcome of the DR process is different for the two ions. For CO_2^+, the following channels can be considered at $E_{rel}=0$:

$$CO_2^+ + e^- \rightarrow \begin{cases} CO_2, & \Delta E = 13.8 \text{ eV} \quad (N_a), \\ C + O_2, & \Delta E = 2.3 \text{ eV} \quad (N_b), \\ CO + O, & \Delta E = 8.3 \text{ eV} \quad (N_c), \\ C + O + O, & \Delta E = -2.8 \text{ eV} \quad (N_d), \end{cases} \tag{7}$$

where ΔE is the kinetic-energy release for production of ground-state fragments. Note that the three-particle break-up channel (d) is energetically closed. For CO_2^{2+}, the situation is somewhat different. As with CO_2^+, we only observe single capture of electrons, which—contrary to the mono cation—leaves charged fragments. Further, several dissociative excitation channels are energetically allowed even at $E_{rel}=0$:

$$CO_2^{2+} + e^- \rightarrow \begin{cases} O_2 + C^{2+} + e^-, & \Delta E = -9.9 \text{ eV} \\ O_2 + C^+, & \Delta E = 14.4 \text{ eV} \quad (N_a), \\ O + O + C^{2+} + e^-, & \Delta E = -15.1 \text{ eV} \\ O + O + C^+, & \Delta E = 9.3 \text{ eV} \quad (N_b), \\ CO + O^{2+} + e^-, & \Delta E = -17.0 \text{ eV} \\ CO + O^+, & \Delta E = 18.1 \text{ eV} \quad (N_c), \\ O + C + O^{2+} + e^-, & \Delta E = -28.2 \text{ eV} \\ O + C + O^+, & \Delta E = 6.9 \text{ eV} \quad (N_d), \\ O + C^+ + O^+ + e^-, & \Delta E = 4.3 \text{ eV} \\ O + CO^{2+} + e^-, & \Delta E = -9.6 \text{ eV} \\ O + CO^+, & \Delta E = 17.7 \text{ eV} \quad (N_e), \\ C + O^+ + O^+ + e^-, & \Delta E = 6.7 \text{ eV} \\ C + O_2^{2+} + e^-, & \Delta E = -10.4 \text{ eV} \\ C + O_2^+, & \Delta E = 13.6 \text{ eV} \quad (N_f). \end{cases} \tag{8}$$

As expected, the DR of a doubly charged system releases on average more kinetic energy than the singly charged equivalent.

From the SSD output (Fig. 2) it is not possible to distinguish between for instance channels a and b in Eq. (8). Both reactions will produce an event in the peak corresponding to two oxygen atoms hitting the detector. If, however, we insert a mesh grid of known transmission T in front of the detector, the two channels a and b will contribute to the double oxygen peak with different probabilities T and T^2. The grid thus differentiates between different channels that would otherwise deposit the same energy in the solid-state detector. As an example from the CO_2^+ system [Eq. (7)], the full energy peak of the SSD spectrum contains contributions from the channels $a, \ldots, d$ as follows:

$$R_{COO} = [aT + bT^2 + cT^2 + dT^3]R_0, \tag{9}$$

where R_{COO} is the rate of events detected in the full energy peak, and R_0 is the total rate of events. Similar equations can be formed for the four remaining peaks in the SSD spectrum.

In our experiment we used two grids of transmissions $\sim 68\%$ and $\sim 24\%$. These transmissions have been determined in previous experiments [39], and repeated analysis shows that the branching ratios are quite insensitive to changes in the transmission values. We thus obtain 16 equations [equations from each of the five peaks with three values (100%, 68%, and 24%) of T, and $a+b+c=1$] and 3 unknowns (a,b,c). This overdetermined system of equations is solved using a standard χ^2 minimization routine.

For CO_2^+, we found the signal in each peak by fitting Gaussian functions to the SSD pulse height spectra in Fig. 2, and from these the branching ratios were calculated. The result for $E_{rel}=0$ is given in Table II.

TABLE II. Result of branching ratio analysis for CO_2^+.

a	b	c
$(4\pm3)\%$	$(9\pm3)\%$	$(87\pm4)\%$

The branching ratios clearly show that channel c (CO + O breakup) is dominant at low energy with channel b contributing a little. This is interesting, because the linear O-C-O molecule thus may break up into a O_2 molecule. The recombination energy of CO_2^+ is much more than the dissociation energy of the molecule, and thus channel a is believed to be 0. This is consistent with the present result within the error bars. Furthermore, nondissociative recombination has to our knowledge so far never been observed in any experiment.

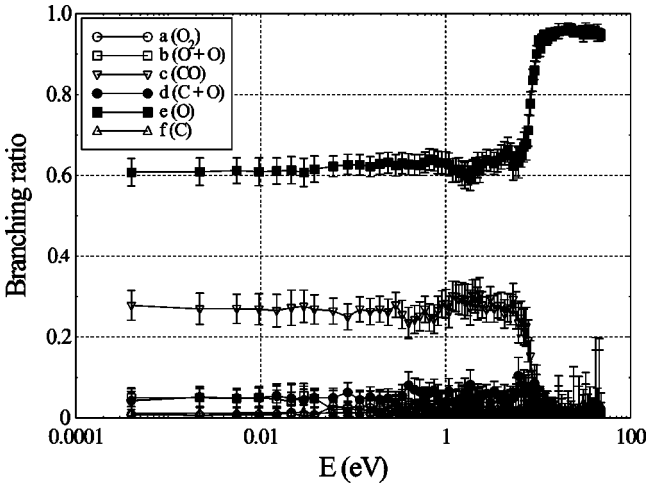

FIG. 5. Dissociative recombination and dissociative excitation branching ratios of CO_2^{2+}. The branching ratios for the six reaction channels listed in Eq. (8) are measured as a function of the relative electron-ion energy.

For CO_2^{2+}, the peaks from the SSD were so well resolved that we could use our standard data acquisition system (using single-channel analyzers) to count the signal events in all peaks. This allowed us to calculate branching ratios as a function of relative energy. The branching ratios are seen in Fig. 5. The DR process appears to result in mainly two channels; *c* (CO production) and *e* (O production). The latter dominates at all energies, but it abruptly increases to almost 100% just below 10 eV. As seen in Eq. (8), this could be the result of the opening of the $O+CO^{2+}$ dissociative excitation channel.

CONCLUSION

To summarize, we have measured dissociative recombination cross sections for CO_2^+ and CO_2^{2+} in the energy range from 10^{-3} eV to 10^1 eV. From these data, thermal rate coefficients of the same magnitude are extracted. Further, product branching ratios have been measured for both ions near zero center-of-mass energy, and for the CO_2^{2+} ion in the energy range from 10^{-3} eV to 50 eV. CO+O breakup is dominant for DR of CO_2^+, while neutral O is the main product of dissociative excitation and recombination of CO_2^{2+}. The measured thermal rate coefficient of CO_2^{2+} DR has recently been applied in calculations, predicting a CO_2^{2+} ion layer in the atmosphere of Mars [20].

ACKNOWLEDGMENTS

This work has been supported by the Danish National Research Foundation through the Aarhus Center for Atomic Physics (ACAP) and by the IHP Program of the EC under Contract No. HPRN CT-2000-00142. We thank the staff at ASTRID for their valuable assistance during the experiments. A.A.K. wishes to thank The Swedish Foundation for International Cooperation in Research and Higher Education.

[1] D.R. Bates, Phys. Rev. **78**, 492 (1950).
[2] J.N. Bardsley, J. Phys. B **1**, 365 (1968).
[3] D. Kella, P.J. Johnson, H.B. Pedersen, L. Vejby-Christensen, and L.H. Andersen, Science **276**, 1530 (1997).
[4] J.L. Fox and F.M. Bakalian, J. Geophys. Res. [Space Phys.] **106**, 28 785 (2001).
[5] J.B.A. Mitchell, in *Dissociative Recombination: Theory, Experiment and Applications III*, edited by D. Zajfman, J.B.A. Mitchell, D. Schwalm, and B.R. Rowe (World Scientific, Singapore, 1996).
[6] David Smith, Chem. Rev. (Washington, D.C.) **92**, 1473 (1992).
[7] A. Sternberg and A. Dalgarno, Astrophys. J., Suppl. Ser. **99**, 565 (1995).
[8] E. Herbst and H.-H. Lee, Astrophys. J. **485**, 689 (1997).
[9] R.J. Oliversen, N. Doane, F. Scherb, W.M. Harris, and J.P. Morgenthaler, Astrophys. J. **581**, 770 (2002).
[10] J.N. Bardsley and M.A. Biondi, Adv. At. Mol. Phys. **6**, 1 (1970).
[11] J. Brian and A. Mitchell, Phys. Rep. **186**, 5 (1990).
[12] M. Larsson, Annu. Rev. Phys. Chem. **48**, 151 (1997).
[13] F.W. Aston, Philos. Mag. **40**, 628 (1920).
[14] R. Conrad, Phys. Z. **31**, 888 (1930).
[15] D. Mathur, Phys. Rep. **225**, 193 (1993).
[16] M. Larsson, Comments At. Mol. Phys. **29**, 39 (1993).
[17] S.S. Prasad and D.R. Furman, J. Geophys. Res. **80**, 1360 (1975).
[18] S. Leach, J. Electron Spectrosc. Relat. Phenom. **41**, 427 (1986).
[19] E.L.O. Bakes, A.G.G.M. Tielens, and C.W. Bauschlicher, Jr., Astrophys. J. **506**, 501 (2001).
[20] O. Witasse, O. Dutuit, J. Lilensten, R. Thissen, J. Zabka, C. Alcaraz, P.-L. Blelly, S.W. Bougher, S. Engel, L.H. Andersen, and K. Seiersen, Geophys. Res. Lett. **29**, 104 (2002).
[21] S.A. Sandford, M.P. Bernstein, L.J. Allamandola, D. Goorvitch, and T.C.V.S. Teixeira, Astrophys. J. **548**, 836 (2001).
[22] D. Talbi and E. Herbst, Astron. Astrophys. **386**, 1139 (2002).
[23] J.J. Thomson, *Rays of Positive Electricity and their Application to Chemical Analysis*, 2nd ed. (Longmans, Green and Co., London, 1921).
[24] A.S. Newton and A.F. Sciamanna, J. Chem. Phys. **40**, 718 (1964).
[25] L.H. Andersen, J.H. Posthumus, O. Vahtras, H. Ågren, N. Elander, A. Nunez, A. Scrinzi, M. Natiello, and M. Larsson, Phys. Rev. Lett. **71**, 1812 (1993).
[26] D. Mathur, L.H. Andersen, P. Hvelplund, D. Kella, and C.P. Safvan, J. Phys. B **28**, 3415 (1995).
[27] J.S. Wright, D.J. Carpenter, A.B. Alekseyev, H-P. Liebermann, R. Lingott, and R.J. Buenker, Chem. Phys. Lett. **266**, 391 (1997).
[28] S. Rosén, R. Peverall, M. Larsson, A. Le Padellec, J. Semaniak, Å. Larson, C. Strömholm, W.J. van der Zande, H. Danared, and G.H. Dunn, Phys. Rev. A **57**, 4462 (1998).
[29] C.P. Safvan, M.J. Jensen, H.B. Pedersen, and L.H. Andersen, Phys. Rev. A **60**, R3361 (1999); **62**, 019901(E) (2000).
[30] S.P. Møller, in *IEEE Particle Accelerator Conference*, edited by K. Berkner (IEEE, New York, 1991).
[31] K.O. Nielsen, Nucl. Instrum. **1**, 289 (1957).
[32] L.H. Andersen, J. Bolko, and P. Kvistgaard, Phys. Rev. A **41**, 1293 (1990).
[33] F. Abildskov and S.P. Møller, in *Beam Instrumentation: Proceedings of the Seventh Workshop*, edited by A.H. Lumpkin and C.E. Eyberger (AIP, New York 1997), pp. 536–543.
[34] P.M. Mul, J.Wm. McGowan, P. Defrance, and J.B.A. Mitchell, J. Phys. B **16**, 3099 (1983), the cross sections in this paper are to be divided by a factor of 2.
[35] C.S. Weller and M.A. Biondi, Phys. Rev. Lett. **19**, 59 (1967).
[36] R.A. Gutcheck and E.C. Zipf, J. Geophys. Res. **78**, 5429 (1973).
[37] M. Geoghegan, N.G. Adams, and D. Smith, J. Phys. B **24**, 2589 (1991).
[38] T. Gougousi, M.F. Golde, and R. Johnsen, Chem. Phys. Lett. **265**, 399 (1997).
[39] M.J. Jensen, R.C. Bilodeau, C.P. Safvan, K. Seiersen, and L.H. Andersen, Astrophys. J. **543**, 764 (2000).